Proc. Natl. Acad. Sci. USA
Vol. 91, pp. 1475–1479, February 1994
Pharmacology

Tityustoxin Kα blocks voltage-gated noninactivating K^+ channels and unblocks inactivating K^+ channels blocked by α-dendrotoxin in synaptosomes

ROBERT S. ROGOWSKI*, BRUCE K. KRUEGER*, JOHN H. COLLINS†‡, AND MORDECAI P. BLAUSTEIN*§

Departments of *Physiology, †Biological Chemistry, and §Medicine, University of Maryland School of Medicine, and the ‡Medical Biotechnology Center of the Maryland Biotechnology Institute, Baltimore, MD 21201

Communicated by William A. Catterall, September 1, 1993

ABSTRACT **Two nonhomologous polypeptide toxins, tityustoxin Kα (TsTX-Kα) and tityustoxin Kβ (TsTX-Kβ), purified from the venom of the Brazilian scorpion *Tityus serrulatus*, selectively block voltage-gated noninactivating K^+ channels in synaptosomes (IC_{50} values of 8 nM and 30 nM, respectively). In contrast, α-dendrotoxin (α-DTX) and charybdotoxin (ChTX) block voltage-gated inactivating K^+ channels in synaptosomes (IC_{50} values of 90 nM and 40 nM, respectively). We studied interactions among these toxins in ^{125}I-α-DTX binding and ^{86}Rb efflux experiments. Both TsTX-Kα and ChTX completely displaced specifically bound ^{125}I-α-DTX from synaptic membranes, but TsTX-Kβ had no effect on bound α-DTX. TsTX-Kα and TsTX-Kβ blocked the same noninactivating component of 100 mM K^+-stimulated ^{86}Rb efflux in synaptosomes. Both α-DTX and ChTX blocked the same inactivating component of the K^+-stimulated ^{86}Rb efflux in synaptosomes. Both the inactivating and the noninactivating components of the 100 mM K^+-stimulated ^{86}Rb efflux were completely blocked when 200 nM TsTX-Kβ and either 600 nM α-DTX or 200 nM ChTX were present. The effects of TsTX-Kα and ChTX on ^{86}Rb efflux were also additive. When TsTX-Kα was added in the presence of α-DTX, however, only the noninactivating component of the K^+-stimulated efflux was blocked. The inactivating component could then be blocked by ChTX, which is structurally homologous to TsTX-Kα. We conclude that TsTX-Kα unblocks the voltage-gated inactivating K^+ channels in synaptosomes when they are blocked by α-DTX, but not when they are blocked by ChTX. TsTX-Kα binds to a site on the inactivating K^+ channel that does not occlude the pore; its binding apparently prevents α-DTX (7054 Da), but not ChTX (4300 Da), from blocking the pore. The effects of TsTX-Kα on ^{125}I-α-DTX binding and ^{86}Rb efflux are mimicked by noxiustoxin, which is homologous to TsTX-Kα and ChTX.**

K^+ channels with distinctive activation–inactivation properties and pharmacological sensitivities play critical physiological roles in many types of cells. The study of these channels and their physiological effects has been aided by the identification of a number of small polypeptides from the venoms of scorpions and snakes that block particular types of K^+ channels with high selectivity and affinity (1–3). For example, α-dendrotoxin (α-DTX), from the venom of the Eastern green mamba, *Dendroaspis angusticeps* (4), selectively blocks voltage-gated inactivating K^+ channels in synaptosomes (5). Venoms from several Old World scorpions also contain polypeptides that block only voltage-gated inactivating K^+ channels (6), although some toxins from *Leiurus quinquestriatus hebraeus*,—notably, charybdotoxin (ChTX)—block high-conductance ("maxi") Ca^{2+}-activated K^+ channels (7) as well as voltage-gated inactivating K^+ channels (6, 8, 9). In contrast, venoms from several New World scorpions contain polypeptides that selectively block only voltage-gated, noninactivating K^+ channels (6). The present report describes an interaction between α-DTX and one of the voltage-gated noninactivating K^+ channel blockers from the Brazilian scorpion *Tityus serrulatus*, tityustoxin Kα (TsTX-Kα).

The publication costs of this article were defrayed in part by page charge payment. This article must therefore be hereby marked "*advertisement*" in accordance with 18 U.S.C. §1734 solely to indicate this fact.

METHODS

Toxins. TsTX-Kα and TsTX-Kβ [originally called TsK4 and TsK2 (6)] and ChTX were purified as described (6, 7). Noxiustoxin (NTX), from the Mexican scorpion *Centruroides noxius*, was a gift from L. D. Possani (Inst. Biotec., UNAM, Cuernevaca, Mexico) and J. S. Smith (Merck Sharp & Dohme Research Labs, West Point, PA). α-DTX was purified from the venom of *D. angusticeps* (5). ^{125}I-α-DTX was prepared as described (10).

The amino acid sequences of TsTX-Kα and TsTX-Kβ were determined by automated Edman degradation. Cysteine residues were identified unambiguously as blank cycles during the sequencer run; all other amino acids yielded identifiable derivatives. The TsTX-Kα sequence was confirmed by expression of active toxin by recombinant DNA methods (11).

Experimental Procedures. The rat brain synaptosome $^{86}Rb^+$ efflux assay was used to study K^+ channel activity (6). The assay for specific binding of ^{125}I-α-DTX to its receptor on rat brain synaptic membranes has been published (10).

The standard (5K) incubation solution was 145 mM NaCl/5 mM KCl/0.1 mM RbCl/2 mM $MgCl_2$/10 mM glucose/0.5 mM NaH_2PO_4/10 mM Hepes adjusted to pH 7.4 with NaOH. The depolarizing (100K) solution contained 100 mM KCl and only 50 mM NaCl.

RESULTS

TsTX-Kα and TsTX-Kβ Block Delayed Rectifier K^+ Channels; α-DTX and ChTX Block A-Type K^+ Channels. Depolarization of $^{86}Rb^+$-loaded synaptosomes with Ca^{2+}-free, K^+-rich medium evokes a large increase in $^{86}Rb^+$ efflux (ΔK) whose three components can readily be identified in time-course experiments (Fig. 1*A*) (6). The K^+-stimulated increase in the (extrapolated) ordinate intercept of the efflux curve corresponds to a component that inactivates within 1 sec. This component represents voltage-gated inactivating (possibly "A-type") K^+ channels (6, 12). The increase in the slope of the curve (relative to the efflux into 5K solution) includes two components that do not inactivate within 5 sec and that are approximately equal in magnitude in 100K solution at 5 sec (6, 12): One noninactivating component is due to the increase in electrodiffusion that results from the depolarization: the second corresponds to an increase in K^+ conductance via voltage-gated noninactivating (possibly

Abbreviations: α-DTX, α-dendrotoxin; ChTX, charybdotoxin; NTX, noxiustoxin; TsTX, tityustoxin.

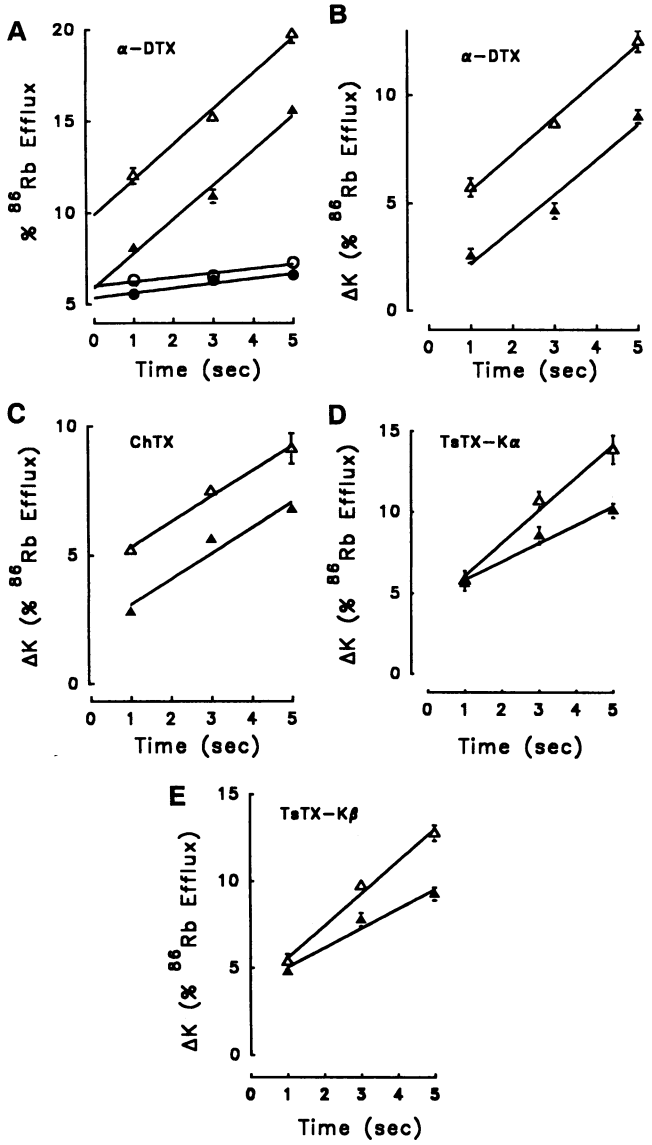

FIG. 1. Time course of $^{86}Rb^+$ efflux in synaptosomes illustrating the effects of several polypeptide toxins. (*A*) Experiment with 600 nM α-DTX. Circles, efflux in 5K; triangles, efflux in 100K; open symbols, toxins absent; filled symbols, toxins present. Symbols indicate means of four replicates; SE bars in this and subsequent figures are shown where they extend beyond the symbols. See ref. 6 for methodological details. (*B–E*) Effects of 600 nM α-DTX, 100 nM ChTX, 30 nM TsTX-Kα, and 200 nM TsTX-Kβ, respectively, on the Ca^{2+}-independent 100K-stimulated $^{86}Rb^+$ efflux (ΔK = efflux into Ca^+-free 100K minus the efflux into Ca^{2+}-free 5K).

"delayed rectifier") K^+ channels. The latter can be blocked by K^+ channel inhibitors such as 4-aminopyridine (8, 13) and by several neurotoxins from New World scorpions (6), but not by α-DTX (5) or ChTX (6, 8).

Fig. 1 illustrates the selective block of the inactivating K^+ channel (i.e., reduction in the Rb^+ efflux ordinate intercept) by 600 nM α-DTX (*A* and *B*) and 100 nM ChTX (*C*) and of the noninactivating K^+ channel (i.e., reduction of the slope of the efflux curve) by 30 nM TsTX-Kα (*D*) and 200 nM TsTX-Kβ (*E*). These toxin concentrations are maximally effective. Both TsTX-Kα and TsTX-Kβ reduced the 100K-induced increase in the slope by about 50%; thus, at 100 mM K^+, about half of the increase in slope can be attributed to the voltage-gated noninactivating K^+ channels and about half to electrodiffusion (12). Voltage-clamp experiments on cultured rat brain neurons confirmed that TsTX-Kα selectively blocks voltage-gated noninactivating (delayed rectifier) K^+ channels with high affinity (14).

Interaction of TsTX-Kα, but Not TsTX-Kβ, with α-DTX Receptor Binding. This distinction between the effects of the two *Tityus* toxins on the noninactivating K^+ channels (Fig. 1 *D* and *E*) and the effects of α-DTX and ChTX on the inactivating K^+ channels (Fig. 1 *A–C*), led us to anticipate that the *Tityus* toxins would not affect inactivating K^+ channels. We therefore compared the effects of these four toxins on the binding of ^{125}I-α-DTX to its receptor site on synaptic membranes. The two inactivating K^+ channel blockers, ChTX and (unlabeled) α-DTX inhibited ^{125}I-α-DTX binding but, unexpectedly, so did the noninactivating channel blocker TsTX-Kα, whereas TsTX-Kβ was ineffective (Fig. 2*A*). The IC_{50} for inhibition of ^{125}I-α-DTX binding by TsTX-Kα was 3 nM (Fig. 2*B*) which is close to its IC_{50} for block of noninactivating K^+ channels, 7 nM (6).

The kinetics of inhibition of ^{125}I-α-DTX binding by TsTX-Kα and by (unlabeled) α-DTX and ChTX were different, however. As expected, unlabeled α-DTX was a competitive inhibitor: it increased the apparent dissociation constant, K_d, but did not affect the maximum binding capacity, B_{max}, (10). ChTX appeared to be a noncompetitive, allosteric inhibitor of α-DTX binding (Fig. 2*C*); it had no effect on the apparent affinity for ^{125}I-α-DTX (i.e., K_d was unchanged) but reduced B_{max}. In contrast, TsTX-Kα both reduced B_{max} and increased K_d (Fig. 2*D*).

Interactions Between α-DTX and TsTX-Kα on Rb^+ Efflux. This evidence that TsTX-Kα displaced α-DTX from its binding site (Fig. 2) but did not block the inactivating K^+ channels (Fig. 1) implied that TsTX-Kα should prevent α-DTX from blocking the inactivating channels. This expectation was tested and verified (Figs. 3 and 4).

The ΔK at 5 sec consists of three approximately equal components which correspond, respectively to the inactivating K^+ channels, the noninactivating K^+ channels, and electrodiffusion (see above). The blocker of the inactivating channels, α-DTX (Fig. 3*A*, ●) blocked about one-third of ΔK, and the blockers of the noninactivating K^+ channels, TsTX-Kα (▲) and TsTX-Kβ (■), also blocked about one-third of ΔK in the absence of α-DTX. Further, the effects of TsTX-Kβ and α-DTX were additive. The residual ΔK in the presence of maximal doses of these two toxins (about 35% of control ΔK) corresponds to the aforementioned electrodiffusion component.

In contrast to TsTX-Kβ (Fig. 3*A*, ■), TsTX-Kα prevented α-DTX from inhibiting the $^{86}Rb^+$ efflux (▲). This lack of effect of α-DTX in the presence of TsTX-Kα cannot be explained by a common site of action, because α-DTX and TsTX-Kα block different channels (Figs. 1 *B* and *D*). Also, TsTX-Kβ did not inhibit the Rb^+ efflux further when added in the presence of saturating concentrations of both α-DTX and TsTX-Kα (Fig. 3*B*). These results indicate that TsTX-Kα prevented α-DTX from blocking the inactivating channels and that α-DTX did not prevent TsTX-Kα from blocking the noninactivating K^+ channels.

More direct evidence that TsTX-Kα, but not TsTX-Kβ, relieves the block of voltage-gated inactivating K^+ channels by α-DTX was provided by the Rb^+ efflux time course. The effects of α-DTX and TsTX-Kβ were additive: TsTX-Kβ alone (Fig. 4*A*) reduced the slope of the ΔK curve (i.e., it blocked the noninactivating channels); addition of α-DTX then reduced the ordinate intercept with no further effect on the slope (i.e., it blocked the inactivating channels). Conversely, α-DTX blocked the inactivating channels and addition of TsTX-Kβ then also blocked the noninactivating channels (Fig. 4*B*). In contrast, when TsTX-Kα was added after α-DTX (Fig. 4*C*), the K-stimulated Rb^+ efflux at 1 sec increased markedly, relieving the inhibition of the inactivating channels by α-DTX; this is reflected in the increase in ordinate intercept (arrow in Fig. 4*C*). The independent effect

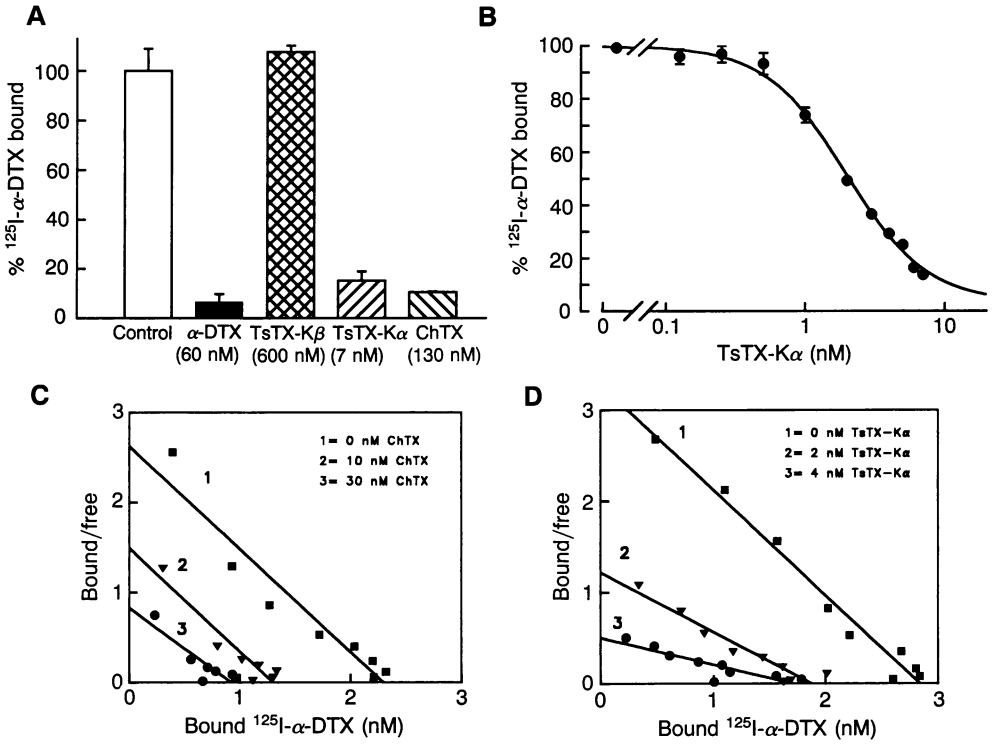

FIG. 2. Effects of scorpion toxins on binding of ^{125}I-α-DTX to synaptic membranes. Error bars in *A* and *B* correspond to SEs of the means of three determinations. All samples (*A–D*) were incubated with the labeled toxin for 30 min to assure equilibrium binding (10). (*A*) Displacement of ^{125}I-α-DaTX bound to synaptic plasma membranes by unlabeled α-DaTX (60 nM), TsTX-Kβ (600 nM), TsTX-Kα (7 nM), and ChTX (130 nM). (*B*) Effect of increasing concentrations of TsTX-Kα on the binding of ^{125}I-α-DaTX binding to synaptic membranes. (*C* and *D*) Scatchard plots of the inhibition of ^{125}I-α-DaTX binding to synaptic membranes by increasing concentrations of ChTX (*C*) and TsTX-Kα (*D*). ^{125}I-α-DaTX binding to synaptic membranes was measured by competitive displacement with increasing concentrations of unlabeled α-DaTX in the presence of (curves 1, 2, and 3, respectively) 0, 10, and 30 nM ChTX (*C*), and 0, 2, and 4 nM TsTX-Kα (*D*). Data points are the means of triplicate determinations. ChTX at 10 and 30 nM decreased B_{max} from the control value of 0.9 to 0.5 and 0.3 pmol/mg of protein, respectively. However, ChTX had no effect on the apparent K_d. TsTX-Kα at 2 and 4 nM also decreased B_{max} from the control value of 2.8 to 1.9 and 1.6 pmol/mg of protein, respectively, but, in addition, TsTX-Kα increased K_d from the control value of 0.8 nM to 1.4 and 2.5 nM, respectively.

of TsTX-Kα on the noninactivating channels is indicated by the reduced slope of the ΔK curve. Thus, only the voltage-gated noninactivating K^+ channels were blocked. Note that the kinetics of $^{86}Rb^+$ efflux in the presence of α-DTX and TsTX-Kα (Fig. 4*C*, ●) were identical to those observed with TsTX-Kα alone (Fig. 1*D*).

Structure–Activity Relationships of Three Homologous Scorpion Toxins. Fig. 5*A* shows the amino acid sequences of ChTX (17), TsTX-Kα (this report), and NTX (noxiustoxin; refs. 13 and 15), and the partial sequence of the larger, nonhomologous TsTX-Kβ (8,016 Da; ref. 6). α-DTX (7054 Da) is a nonhomologous polypeptide (5). ChTX, TsTX-Kα, and NTX share substantial sequence homology, especially at their C termini; they also have three similarly positioned cysteine residues, which suggests that they are similarly folded via disulfide bridges. Nevertheless, both TsTX-Kα

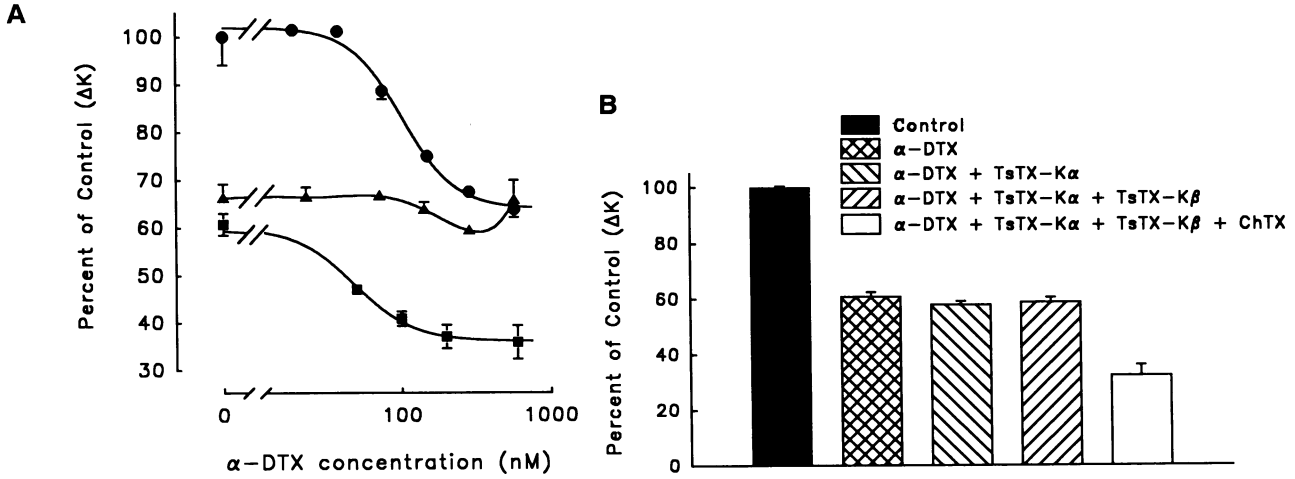

FIG. 3. (*A*) Dose–response curves showing block of the Ca^{2+}-independent 5-sec ΔK from rat brain synaptosomes by α-DaTX alone (●) or in the presence of 80 nM TsTX-Kα (▲) or 200 nM TsTX-Kβ (■). Symbols correspond to differences between the means of four determinations each in 5K and 100K. (*B*) Effects on the 5-sec ΔK of 600 nM α-DTX alone or in the presence of 80 nM TsTX-Kα, 80 nM TsTX-Kα plus 200 nM TsTX-Kβ, or 80 nM TsTX-Kα plus 200 nM TsTX-Kβ plus 200 nM ChTX.

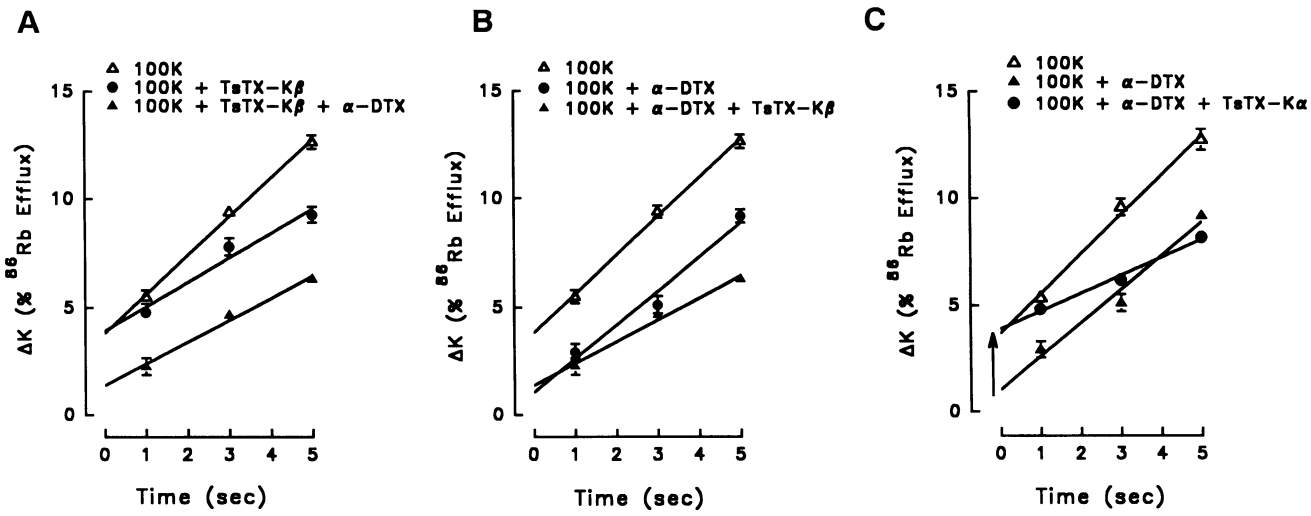

FIG. 4. Time course of the effects of 200 nM TsTX-Kβ alone (●) and in the presence of 600 nM α-DaTX (▲) (*A*), of 600 nM α-DTX alone (●) and in the presence of 200 nM TsTX-Kβ (▲) (*B*), and 600 nM α-DTX alone (▲) and in the presence of 80 nM TsTX-Kα (●) (*C*) on the Ca^{2+}-independent 100K-stimulated Rb^+ efflux (ΔK) in synaptosomes. △, Control 100K-stimulated Rb^+.

and NTX block noninactivating, and not inactivating, K^+ channels, whereas the opposite is true for ChTX (6, 8).

TsTX-Kβ and α-DTX, like the three small scorpion toxins, contain many positively charged residues. Also, α-DTX contains three disulfide bridges.

The time course (Fig. 5*B*) demonstrates that NTX also prevented α-DTX from blocking the inactivating K^+ channels. NTX also completely displaced specifically bound ^{125}I-α-DTX from synaptic membranes (not shown). Thus, NTX is both structurally and functionally similar to TsTX-Kα.

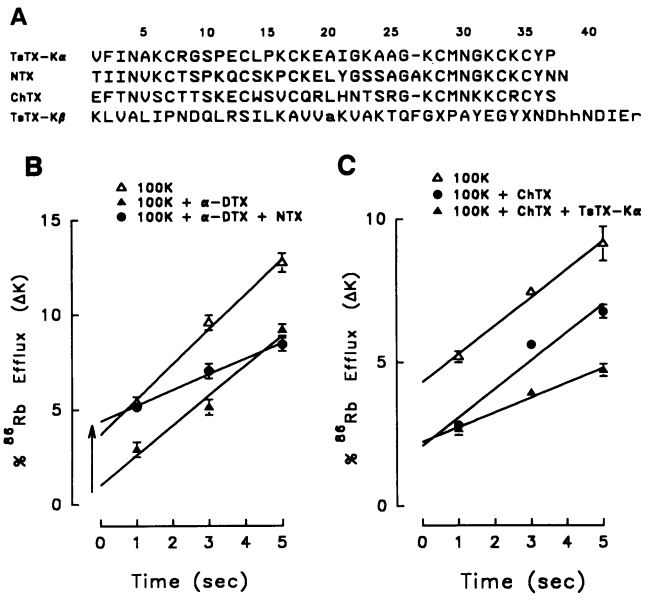

FIG. 5. (*A*) Amino acid sequences of TsTX-Kα (3997 Da), NTX (4184 Da) (13, 15), and ChTX (4300 Da) (8). The toxins are aligned so that their cysteines lie in identical positions. ChTX contains three disulfide bridges (Cys^7–Cys^{28}, Cys^{13}–Cys^{33}, and Cys^{17}–Cys^{35}; ref. 16); we assume that TsTX-Kα and NTX contain the same disulfide bridges. The partial sequence (first 45 amino acids) of the nonhomologous TsTX-Kβ (≈8160 Da; ref. 6) is also shown. Lowercase letter indicates tentative identification; X, unidentified amino acid. (*B*) Time course of the effects on ΔK of 600 nM α-DTX alone (▲) and in the presence of 300 nM NTX (●). (*C*) Time course of the effects on ΔK of 200 nM CTX alone (●) and in the presence of 80 nM TsTX-Kα (▲).

Even though TsTX-Kα and ChTX are homologous (Fig. 5*A*), and ChTX and α-DTX interact at the α-DTX binding site on synaptic membranes (Fig. 2), TsTX-Kα did not prevent the block of the inactivating K^+ channels by ChTX. The effects of ChTX and TsTX-Kα were additive (Fig. 5*C*). Thus, the inactivating channels as well as the noninactivating channels were blocked in the presence of these two toxins.

While both TsTX-Kβ and TsTX-Kα blocked the noninactivating K^+ channels, TsTX-Kβ did not prevent TsTX-Kα from relieving the α-DTX block of the inactivating channels (Fig. 3*B*). Further, in the presence of α-DTX, TsTX-Kα, and TsTX-Kβ, ChTX was still able to block the inactivating channels (Fig. 3*B*) even though, in the absence of TsTX-Kα (and TsTX-Kβ), the effects of α-DTX and ChTX are not additive (6).

DISCUSSION

This report describes an unanticipated interaction between two nonhomologous polypeptide K^+ channel toxins. TsTX-Kα selectively blocks voltage-gated noninactivating (possibly delayed rectifier) K^+ channels in synaptosomes (6). α-DTX selectively blocks voltage-gated inactivating (possibly A-type) K^+ channels (6). Our data show that TsTX-Kα interferes with the binding of α-DTX to its receptor and thereby unblocks α-DTX-blocked inactivating channels even though TsTX-Kα does not itself block these channels. However, the block of the inactivating channels by ChTX, which has substantial sequence homology to TsTX-Kα, is not prevented by TsTX-Kα. These effects of TsTX-Kα are mimicked by NTX, a homologous toxin from another New World scorpion. NTX also displaces the α-DTX homologue dendrotoxin I from its receptor on rat brain synaptic membranes (18).

These polypeptide toxins are all hydrophilic and bear a substantial net positive charge; they are all probably too large to cross the plasmalemma (11). ChTX binds in the mouth of Ca^{2+}-activated (19) and voltage-gated (20, 21) K^+ channels. α-DTX also binds to an external site on K^+ channels (21–23), as does TsTX-Kα (11).

Much is known about the binding of ChTX to Ca^{2+}-activated K^+ channels. Three of the toxin's positively charged amino acids (Arg^{25}, Lys^{27}, and Arg^{34}; see Fig. 5*A*) are critical for the electrostatic interaction with the side-chains of amino acids that form the channel mouth (24). Lys^{27} apparently sits close to the K^+ binding site (19) and accounts for

the voltage dependence of the toxin's dissociation (24). This Lys^{27} is present in all of the homologous scorpion K^+ toxins that have been sequenced (Fig. 5*A*; refs. 25–30).

ChTX also binds to and blocks voltage-gated K^+ channels, as discussed above. The negative charge of Glu^{422} in the channel protein's extracellular S5–S6 loop provides a negative electrostatic potential in the mouth of the cloned Shaker B channel. This amino acid is critical for ChTX binding (20).

The α-DTX binding site has been localized to the S5–S6 loop of cloned RBK2 (BK2) channels (22) and RCK1 channels (23). There is disagreement, however about whether the only negatively charged residue in this loop, Glu^{353}, is critical for α-DTX binding (22, 23). Since all identified types of K^+ channels apparently consist of homo- or heterotetramers of comparable ≈60-kDa subunits (31), these data suggest that the S5–S6 loops of the four subunits face the central pore (or conductance pathway) and that together they form the mouth of the pore. The binding sites for the K^+ channel toxins must then be situated on the S5–S6 loops; all four of the loops may contribute to and coordinate the binding of the toxins. However, a single toxin molecule may not need to bind to all four channel subunits to exert its effect; indeed, this might help to explain some of the toxin interactions that we observed.

The binding sites for ChTX and NTX in mouse brain synaptosomes are not identical; ChTX displaces only about one-third of the specifically bound NTX (15). In contrast, ChTX as well as TsTX-Kα (Fig. 2*A*) and NTX (data not shown, but see ref. 18) completely displace specifically bound α-DTX from rat brain synaptic membranes. Our data suggest that the overlap between the ChTX and NTX binding (15) may be on the inactivating K^+ channels, whereas the remainder of the NTX binding sites may be located on the noninactivating channels. Substitution in amino acid position 25 (alanine in NTX and TsTX-Kα, arginine in ChTX) may contribute to the selectivity differences because the positively charged arginine is critical for ChTX binding to its receptor in the high-conductance Ca^{2+}-activated K^+ channel mouth (19).

The work of Miller and MacKinnon and their collaborators (19, 20) and the striking sequence homologies of all the ≈4-kDa scorpion K^+ channel toxins (Fig. 5*A*; refs. 24–29) make it reasonable to speculate that block of the several types of K^+ channels by these toxins may involve similar mechanisms. These toxins may, like ChTX, insert deep into the mouths of the channels, with Lys^{27} situated close to a K^+ binding site in the conductance pathway, thereby physically occluding the pores. Whether TsTX-Kβ and α-DTX, which are substantially larger molecules (≈8 and ≈7 kDa, respectively) plug the pores of voltage-gated noninactivating and inactivating K^+ channels, respectively, in a similar fashion, is not known. However, the fact that ChTX antagonizes the binding of α-DTX, and that both of these toxins block the inactivating channels, suggests that α-DTX also inserts deep into the mouth of this channel. In contrast, TsTX-Kα and NTX must bind to a site distant from the α-DTX binding site on the inactivating channel, because they completely antagonize α-DTX binding and block without themselves plugging the conductance pathway. Thus, they may either prevent α-DTX binding via an allosteric effect or sterically interfere with the access of α-DTX, but not ChTX, to the narrow pore of the channel.

This work was supported by National Institutes of Health Grants RO1-NS16106 (M.P.B.) and RO1-NS16285 (B.K.K.), by a National Institute of Mental Health Grant to the Maryland Psychiatric Research Institute Neuroscience Center for Research in Schizophrenia (P50-MH44211; subproject director, M.P.B.), and by funds from the Medical Biotechnology Center of the Maryland Biotechnology Institute, University of Maryland.

1. Moczydlowski, E., Lucchesi, K. & Ravindran, A. (1989) *J. Membr. Biol.* **105**, 95–111.
2. Strong, P. N. (1990) *Pharmacol. Ther.* **46**, 37–162.
3. Dreyer, F. (1990) *Rev. Physiol. Biochem. Pharmacol.* **115**, 93–136.
4. Harvey, A. L. & Anderson, A. J. (1985) *Pharmacol. Ther.* **31**, 33–55.
5. Benishin, C. G., Sorensen, R. G., Brown, W. E., Krueger, B. K. & Blaustein, M. P. (1988) *Mol. Pharmacol.* **34**, 152–159.
6. Blaustein, M. P., Rogowski, R. S., Schneider, M. J. & Krueger, B. K. (1991) *Mol. Pharmacol.* **40**, 932–942.
7. Miller, C., Moczydlowski, E., Latorre, R. & Phillips, M. (1985) *Nature (London)* **313**, 316–318.
8. Schneider, M. J., Rogowski, R. S., Krueger, B. K. & Blaustein, M. P. (1989) *FEBS Lett.* **250**, 433–436.
9. Schweitz, H., Stansfield, C. E., Bidard, J. N., Fagni, L., Maes, P. & Lazdunski, M. (1989) *FEBS Lett.* **250**, 519–522.
10. Sorensen, R. G. & Blaustein, M. P. (1989) *Mol. Pharmacol.* **36**, 689–698.
11. Werkman, T. R., Gustafson, T. A., Rogowski, R. S., Blaustein, M. P. & Rogawski, M. A. (1993) *Mol. Pharmacol.* **44**, 430–436.
12. Bartschat, D. K. & Blaustein, M. P. (1985) *J. Physiol. (London)* **361**, 419–440.
13. Possani, L. D., Martin, B. M. & Svendsen, I. (1982) *Carlsberg Res. Commun.* **47**, 285–289.
14. Eccles, C. U., Rogowski, R. S., Alger, B. E. & Blaustein, M. P. (1993) *Soc. Neurosci. Abstr.* **19**, 708.
15. Valdivia, H. H., Smith, J. S., Martin, B. M., Coronado, R. & Possani, L. D. (1988) *FEBS Lett.* **226**, 280–284.
16. Sugg, E. E., Garcia, M. L., Reuben, J. P., Pachett, A. A. & Kaczorowski, G. J. (1990) *J. Biol. Chem.* **265**, 18745–18748.
17. Giminez-Gallego, G., Navia, M. A., Reuben, J. P., Katz, G. M., Kaczorowski, G. J. & Garcia, M. L. (1988) *Proc. Natl. Acad. Sci. USA* **85**, 3329–3333.
18. Harvey, A. L., Marshall, D. L. & Possani, L. D. (1992) *Toxicon* **30**, 1497–1500.
19. Park, C.-S. & Miller, C. (1992) *Neuron* **9**, 307–313.
20. MacKinnon, R., Heginbotham, L. & Abramson, T. (1990) *Neuron* **5**, 767–771.
21. Werkman, T. R., Kawamura, T., Yokoyama, S., Higashida, H. & Rogawski, M. A. (1992) *Neuroscience* **50**, 935–946.
22. Hurst, R. S., Busch, A. E., Kavanaugh, M. P., Osborne, P. B., North, R. A. & Adelman, J. P. (1991) *Mol. Pharmacol.* **40**, 572–576.
23. Stocker, M., Pongs, O., Hoth, M., Heinemann, S. H., Stuhmer, W., Schroter, K.-H. & Ruppersberg, J. P. (1991) *Proc. R. Soc. London B* **245**, 101–107.
24. Park, C.-S. & Miller, C. (1992) *Biochemistry* **31**, 7749–7755.
25. Chicchi, G. G., Giminez-Gallego, G., Ber, E., Garcia, M. L., Winquist, R. & Cascieri, M. A. (1988) *J. Biol. Chem.* **263**, 10191–10197.
26. Lucchesi, K., Ravindran, A., Young, H. & Moczydlowski, E. (1989) *J. Membr. Biol.* **109**, 269–281.
27. Galvez, A., Gimenez-Gallego, G., Reuben, J. P., Roy-Constancin, L., Feigenbaum, P., Kaczorowski, G. J. & Garcia, M. L. (1990) *J. Biol. Chem.* **265**, 11083–11090.
28. Novick, J., Leonard, R. J., King, V. F., Schmalhofer, W., Kaczorowski, G. J. & Garcia, M. L. (1991) *Biophys. J.* **59**, 78a.
29. Auguste, P., Hugues, M., Mourre, C., Moinier, D., Tartar, A. & Lazdunski, M. (1992) *Biochemistry* **31**, 648–654.
30. Crest, M., Jacquet, G., Gola, M., Zerrouk, H., Benslimane, A., Rochat, H., Mansuelle, P. & Martin-Eauclaire, M.-F. (1992) *J. Biol. Chem.* **267**, 1640–1647.
31. Jan, L. Y. & Jan, Y. N. (1992) *Annu. Rev. Physiol.* **54**, 537–555.